Dynamic hysteresis and scaling behavior in epitaxial antiferroelectric film

Ge Jun, Ying Chen, Xian-Lin Dong, Denis Remiens, Xin Guo, Fei Cao, Gen-Shui Wang

Thin Solid Films 584 (2015) 108–111

Dynamic hysteresis and scaling behavior in epitaxial antiferroelectric film

Jun Ge [a,b,c], Ying Chen [a], Xianlin Dong [a], Denis Rémiens [b,c], Xin Guo [a], Fei Cao [a], Genshui Wang [a,*]

[a] Key Laboratory of Inorganic Functional Materials and Devices, Shanghai Institute of Ceramics, Chinese Academy of Sciences, 1295 Dingxi Road, Shanghai 200050, People's Republic of China
[b] IEMN-DOAE-MIMM, CNRS UMR 8520, Cité scientifique, 59655 Villeneuve-d'Ascq Cedex, France
[c] Université de Valenciennes et du Hainaut Cambrésis, 59313 Valenciennes Cedex 9, France

Article info

Keyword:
Dynamic hysteresis
Scaling behavior
Antiferroelectric film

Abstract

In this study, we investigated the scaling behavior of dynamic hysteresis with frequency f and electric field E in epitaxial $PbZrO_3$ antiferroelectric film on (111)-oriented $SrTiO_3$ substrate. The scaling relation for the saturated hysteresis loops takes the form of hysteresis area $<A> \propto f^{0.03}(E-499)^{0.20}$ at relatively low testing f. However, when frequency exceeds 30 Hz, the <A> shows stronger dependence on f while remains basically unchanged relation with E, leading to a form of $<A> \propto f^{0.10}(E-499)^{0.20}$. The scaling behavior is modeled as occurring in aviscous medium where several forces, such as viscous and restoring forces, act on the phase transition process.

1. Introduction

Antiferroelectric (AFE) materials are promising candidates of great current interest for future high-energy and fast-speed storage capacitors, due to the field-forced phase transition into the ferroelectric state accompanied by large charge storage [1–5]. Thin films of AFE and ferroelectric (FE) materials are of particular interest due to their relevant applications in connection with microelectronic devices [4,6]. Moreover, antiferroelectric films are believed to contain a much higher energy density than their bulk counterparts because of their much higher breakdown field [7,8].

The energy density that is recoverable after charging an electroceramic material in a capacitor structure can be obtained from hysteresis loops by

$$W = \int_{P_{max}}^{P_r} EdP \text{ (upon discharging)} \quad (1)$$

where E is the electric field, P_r and P_{max} are the remanent polarization and polarization at the highest field, respectively. Hence, the dynamic hysteresis, i.e., hysteresis area <A> as a function of the field amplitude E_0 and frequency f, has become an important consideration [9–11]. Indeed, the material devices are often required to operate under conditions of varying frequencies and electric field in practical applications. Therefore, a prior knowledge of how the material properties change under different operating conditions and establishment of their scaling relation is considerably crucial for the selection of a suitable working condition and the design of a proper energy-storage device. Many theoretical studies have been focused on scaling law $<A> \propto f^{\alpha}E_0^{\beta}$ (where α and β are exponents that depend on the dimensionality and symmetry of the system) of hysteresis curves in polarization systems. In the realm of antiferroelectric, Kim et al. [12] observed the f- and E_0-dependence of the dynamic hysteresis in a AFE betaine phosphate-arsenate ($BP_{0.9}A_{0.1}$) crystal, and found two scaling relations of hysteresis area <A> against f and E_0 at frequency below 200 Hz, i.e.,

$$<A> \propto f^{0.40}(E-E_c)^{0.50} \text{ for saturated loops} \quad (2)$$

$$<A> \propto f^{0.28}(E-E_c)^{2.12} \text{ for minor loops} \quad (3)$$

where E_c is the threshold field for the AFE–FE phase transition.

$PbZrO_3$-based AFE materials are the most studied and promising perovskite AFE materials for energy storage applications. For example, it was reported that a remarkable energy storage density of 14.9 J/cm^3 was obtained in 700-nm-thick La-modified $PbZrO_3$ AFE films [7]. Even higher energy densities of 65 and 56 J/cm^3 have been obtained very recently, in $Pb_{0.92}La_{0.08}(Zr_{0.95}Ti_{0.05})O_3$ and $Pb_{0.97}La_{0.02}(Zr_{0.55}Sn_{0.40}Ti_{0.05})O_3$ AFE films, respectively [3,13]. Among various perovskite AFE materials, lead zirconate $PbZrO_3$ was the first compound that was identified as an antiferroelectric and its behavior is representative of any perovskite AFE. In our previous study, we reported scaling behavior of energy density with f in $PbZrO_3$-based AFE films [9]. However, there has been no report on the scaling studies of AFE hysteresis area in thin films. Thus, we present in this paper the results on the scaling behavior of the dynamic hysteresis of epitaxial $PbZrO_3$ thin film.

* Corresponding author. Tel.: +86 21 52412024; fax: +86 21 52411104.
E-mail address: genshuiwang@mail.sic.ac.cn (G. Wang).

2. Experimental details

A $LaNiO_3$ (LNO) bottom electrode was firstly deposited on single crystal (111) $SrTiO_3$ substrates at 450 °C and 1 Pa of 20% oxygen and 80% argon via radio frequency (RF) magnetron sputtering. ~300-nm-thick $PbZrO_3$ films were then grown by off-axis RF magnetron sputtering using a 3-inch-diameter $PbZrO_3$ target made by uniaxial pressed mixed PbO and ZrO_2 powders in stoichiometric composition. The films were deposited on unheated substrate plate under the total pressure of 1 Pa (100% argon), with an RF-power of 1.32 W/cm^2 and the target–substrate distance is 60 mm. These growth conditions yielded a deposition rate of about 570 Å/h for the $PbZrO_3$ layer. The as-deposited films were amorphous and a post annealing treatment under air atmosphere at 625 °C was performed to crystallize the films into the perovskite phase. The structure and phase purity of the films were checked using Rigaku SmartLab high resolution X-ray diffractometer (HRXRD) equipped with a 9 kW rotating anode X-ray generator (lambda $K_{\alpha 1} = 1.54059$ nm). The X-ray beam was made parallel with crossbeam optics and was monochromatized with a double Ge (220) monochromator. Epitaxial relation with substrate was confirmed by XRD φ scan. (Details of the structure information can be found elsewhere [14].) In order to make the electric experiments, LNO top electrode (diameter of ~140 μm) was deposited by RF magnetron sputtering at RT through a photolithography process. After, the samples were annealed at 450 °C for 1 h to improve the electric conductivity. We deposited six samples in one sputtering using multiple base plates. Then we measured approximately 5 electrodes which were all in the center of sample for each film. The averaged data are presented in this paper. *P*–E hysteresis loops and switching current curves were measured using aixACCT TF Analyzer 2000 (aixACCT Systems GmbH; Dennewartstrasse, Aachen, Germany). The *f* covered from 5 to 2000 Hz and *E* ranged from 667 to 778 kV/cm. The measurements started at low frequencies and low fields, and continued by increasing the frequency and the field amplitude.

3. Results and discussion

The saturated polarization–electric field (*P*–*E*) loop and its corresponding current (*I*)–electric field (*E*) curve at 704 kV/cm and 50 Hz are illustrated in Fig. 1. The film exhibits the AFE nature with a typical double hysteresis loops and four current peaks. The saturated polarization (P_s) reaches ~43 μC/cm^2 while the remanent polarization (P_r) is near zero with a small value around 2 μC/cm^2. The first two current peaks of the *I*–*E* curve, which correspond to the forward switching field E_{AF} and the backward switching field E_{FA}, can be interpreted as

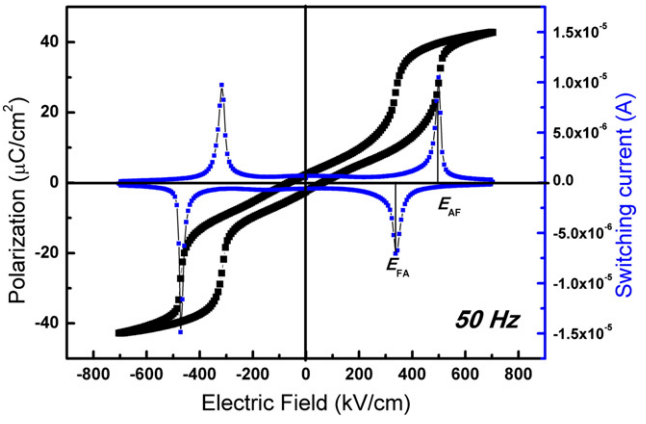

Fig. 1. (color online) Double hysteresis loop and corresponding current curve of $PbZrO_3$ films at ~700 kV/cm and 50 Hz.

AFE–FE and FE–AFE switching fields, respectively. According to the *I*–*E* curve, the values of E_{AF} and E_{FA} are determined to be 499 kV/cm and 337 kV/cm, respectively.

The hysteresis loops of $PbZrO_3$ films at various *E* and *f* are shown in Fig. 2. The hysteresis area <A> increases a little bit with the increase of frequency. The dependence of hysteresis loops on *E* is depicted by comparing loops in different figures. The lowest electric field is set deliberately high enough to avoid the antiferroelectric region, which ensures that the well saturated loops are achieved.

To investigate the scaling behavior, we followed the scaling relations of Eqs. (2) and (3) and fitted these data of double loops with $<A> \propto f^{\alpha}(E - E_{AF})^{\beta}$. To obtain the suitable scaling relation for our film, the *E*-term exponent β is obtained by plotting <A> against $(E_0 - E_{AF})$ at 10 Hz. Similarly, the *f*-term exponent α is obtained by plotting <A> against *f* at fixed field of 667 kV/cm. The data are shown in Fig. 3(a) and the solid line represents a fitting in terms of

$$<A> \propto f^{0.03}(E-499)^{0.20} \quad (4)$$

Clearly, large deviation observed implies that such scaling relation is not applicable to our films. However, a closer look shows that the low *f*-term data can be reasonable fitted (with $R^2 > 0.99$). As the *f* continues to increase, the data deviate from the relation gradually with a higher slope. It is possible that a different scaling behavior might be established for the higher *f*-field region, as reported in previous investigations [11,15].

Here, it should be worthwhile to compare our result with the scaling relations of ferroelectric films. It was reported that a scaling relation as $<A> \propto f^{\alpha}E_0^{\beta}$ was found in $Pb(Zr_{0.52}Ti_{0.48})O_3$ (PZT) ferroelectric thin film at *f* higher than 10 Hz at which α and β are $-1/3$ and 1, respectively [16,17]. Similar phenomena have also been observed in $Pb_{0.9}Ba_{0.1}(Zr_{0.52}Ti_{0.48})O_3$ ferroelectric thin film in which α and β are -0.2 and 2.2, respectively [18]. Clearly, there are large differences in scaling relation between AFE and FE films. It can be seen that the *f* term of our epitaxial $PbZrO_3$ film shows an exponent of 0.03, which is much smaller in absolute value than that of PZT ferroelectric films. To explain the difference, one may need to consider the influence of domain structures on the dynamic hysteresis and scaling behavior. For idea AFE material, the <A> is zero at the region of AFE phase. When electric field excesses the critical point E_{AF}, the AFE–FE phase transition occurs. This accompanies with the formation and growth of FE domains. However, it's worth noting that our electric field *E* is set above 667 kV/cm, which is about 1.3 time of E_{AF}. This implies that the *E* we applied here is high enough to saturate the loops and this can be confirmed by our experiment results with very sharp ending of loops shown in Fig. 2. In such situation, most of the available domains have been switched and the polarization switching is considered to be governed by the irreversible domains. Therefore, lower exponents for the *E* and *f* term are expected from our AFE films. In contrast, we find in other papers which report minus *f* exponents, that the hysteresis loop is not well saturated at some frequencies. Interestingly, similar relations are reported in $Pb(Zr,Ti)O_3$ ferroelectric ceramics where *E* is high enough; hence loops are well saturated, of which α and β are 0.01 and 0.10, respectively [19].

Returning to the observation of Fig. 3(a), there are actually two slopes—one at low frequency *f* and a different slope at relatively high frequency *f* (at different *E* fields). We fit the data with a higher α in terms of:

$$<A> \propto f^{0.10}(E-499)^{0.20} \quad (5)$$

as shown in Fig. 3(b). It is therefore important to explain the fundamental nature of different slopes with *f*. Firstly, we may interpret E_{AF} by the mechanical consideration as an effective field necessary to overcome restoring force (F_R) (turning back to AFE phases) and viscous force (F_V) in domain wall motions [15]. Fig. 4(a) and (b) shows schematically,

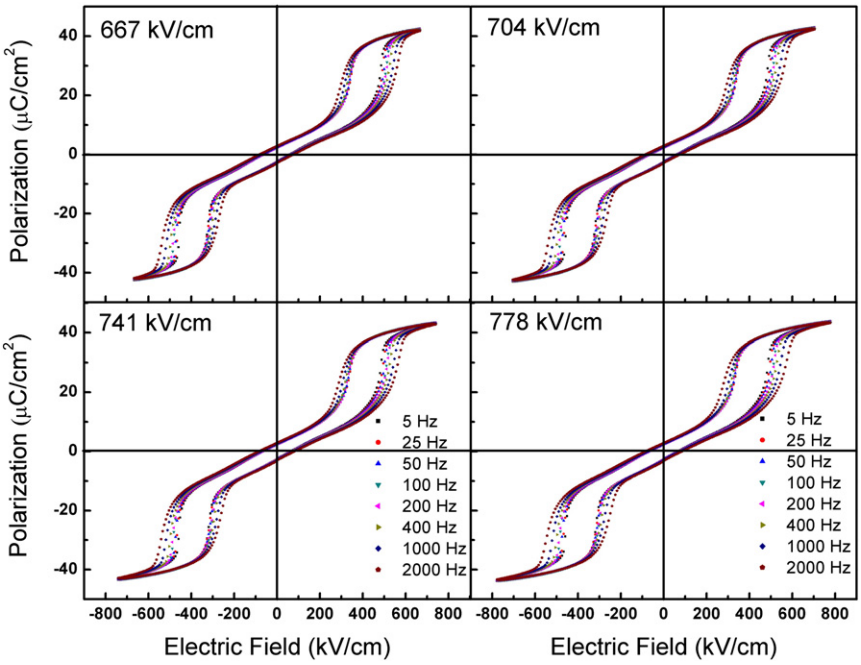

Fig. 2. (color online) Hysteresis loops of $PbZrO_3$ films at various f and E_0 of (a) 667 kV/cm, (b) 704 kV/cm, (c) 741 kV/cm, and (d) 778 kV/cm.

how these forces act on the domains during the application and removal of electric field, respectively. As shown in the figures, the F_V always hinders AFE–FE and FE–AFE phase transition during forward and backward processes, thus increase the E_{AF} and decrease the E_{FA}, respectively. This will lead to an increase in hysteresis area <A>. At lower f, the velocity of the motions is relatively low and F_V could be neglected, and consequently, only F_R and electrical forces act on them. With increasing f, the material becomes more viscous because of the increasing speed of the phase transition movement, and F_V increases accordingly due to their higher velocity; thus this can lead to a higher rate of increase of <A> with f. Furthermore, the F_V apparently is not affected by the magnitude of electric field; hence the relation of <A> with E goes with a constant parameter β.

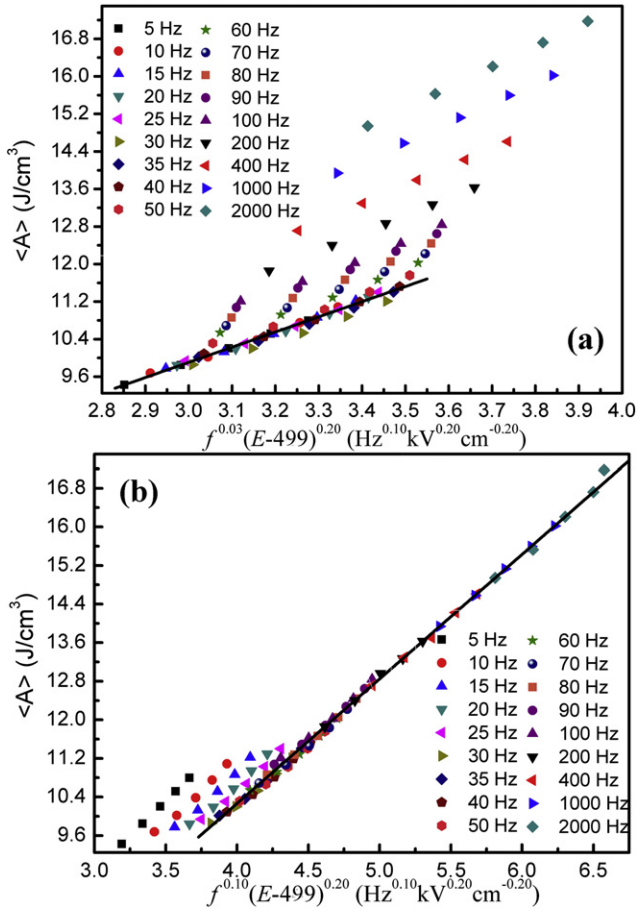

Fig. 3. (color online) Scaling plot of hysteresis area <A> against (a) $f^{0.03}(E-499)^{0.20}$ and (b) $f^{0.10}(E-499)^{0.20}$ for double loops of $PbZrO_3$ films.

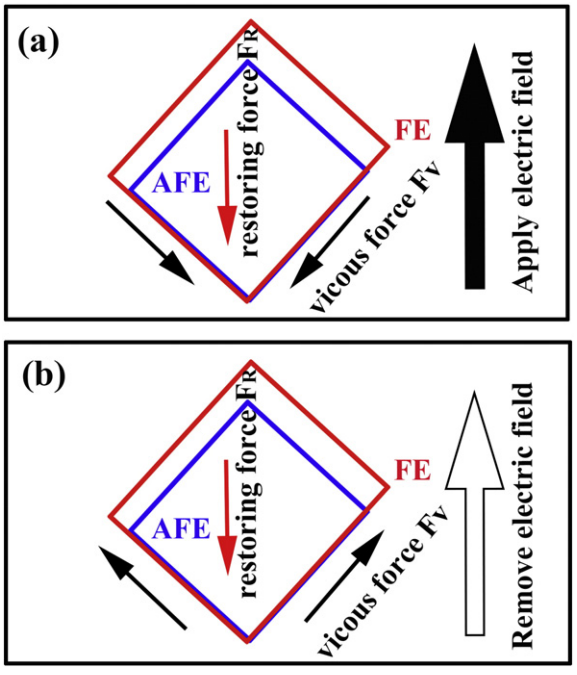

Fig. 4. (color online) Representation of forces acting on phases during the phase transition: (a) during the application of the electric field and (b) during the removal of the field.

4. Conclusions

In summary, the scaling relation for the saturated hysteresis loops of the epitaxial $PbZrO_3$ AFE thin film takes the form of <A> $\propto f^{0.03}(E_0 - E_{AF})^{0.20}$ at relatively low testing frequency f. However, when frequency exceeds 30 Hz, the <A> shows stronger dependence on f while remains basically unchanged relation with E, leading to a form of <A> $\propto f^{0.10}(E_0 - E_{AF})^{0.20}$. As a result, the study provides a detailed understanding of how the <A> of the double loops of AFE thin film behaves in response to various frequency and electric field conditions. We model the dynamic behavior as occurring in a viscous medium where several forces, such as viscous and restoring forces, act on the phase transition process. We find that these relations are closely related to the variation of F_V with the frequency f.

Acknowledgments

The authors would like to thank Dr. Yves Sama and Dr. Pascal Roussel for their support for sputtering process and HRXRD measurements, respectively. This work was supported by NSAF (No.U1330128), the National Important Basic Research Project (2012CB619406), the Shanghai International Science and Technology cooperation project (No. 13520700700), the Open Project Key Laboratory of Polar Materials and Devices Ministry of Education (Grant No. KFKT20120001) and international partnership project of Chinese Academy of Science.

References

[1] K. Yao, S. Chen, M. Rahimabady, M.S. Mirshekarloo, S. Yu, F.E. Tay, T. Sritharan, L. Lu, Nonlinear dielectric thin films for high-power electric storage with energy density comparable with electrochemical supercapacitors, IEEE Trans. Ultrason. Ferroelectr. Freq. Control 58 (2011) 1968.

[2] M. McMillen, A.M. Douglas, T.M. Correia, P.M. Weaver, M.G. Cain, J.M. Gregg, Increasing recoverable energy storage in electroceramic capacitors using "dead-layer" engineering, Appl. Phys. Lett. 101 (2012) 242904.

[3] X. Hao, Y. Wang, L. Zhang, L. Zhang, S. An, Composition-dependent dielectric and energy-storage properties of (Pb, La)(Zr, Sn, Ti)O_3 antiferroelectric thick films, Appl. Phys. Lett. 102 (2013) 163903.

[4] J. Ge, X. Dong, Y. Chen, F. Cao, G. Wang, Enhanced polarization switching and energy storage properties of $Pb_{0.97}La_{0.02}(Zr_{0.95}Ti_{0.05})O_3$ antiferroelectric thin films with $LaNiO_3$ oxide top electrodes, Appl. Phys. Lett. 102 (2013) 142905.

[5] X. Hao, J. Zhai, L.B. Kong, Z. Xu, A comprehensive review on the progress of lead zirconate-based antiferroelectric materials, Prog. Mater. Sci. 63 (2014) 1.

[6] M.S. Mirshekarloo, K. Yao, T. Sritharan, Large strain and high energy storage density in orthorhombic perovskite, $(Pb_{0.97}La_{0.02})(Zr_{1-x-y}Sn_xTi_y)O_3$ antiferroelectric thin films, Appl. Phys. Lett. 97 (2010) 142902.

[7] J. Parui, S.B. Krupanidhi, Enhancement of charge and energy storage in sol-gel derived pure and La-modified $PbZrO_3$ thin films, Appl. Phys. Lett. 92 (2008) 192901.

[8] X. Hao, Z. Yue, J. Xu, S. An, C.-W. Nan, Energy-storage performance and electrocaloric effect in (100)-oriented $Pb_{0.97}La_{0.02}(Zr_{0.95}Ti_{0.05})O_3$ antiferroelectric thick films, J. Appl. Phys. 110 (2011) 064109.

[9] J. Ge, G. Pan, D. Remiens, Y. Chen, F. Cao, X. Dong, G. Wang, Effect of electrode materials on the scaling behavior of energy density in $Pb(Zr_{0.96}Ti_{0.03})Nb_{0.01}O_3$ antiferroelectric films, Appl. Phys. Lett. 101 (2012) 112905.

[10] X. Chen, F. Cao, H. Zhang, G. Yu, G. Wang, X. Dong, Y. Gu, H. He, Y. Liu, Dynamic hysteresis and scaling behavior of energy density in $Pb_{0.99}Nb_{0.02}(Zr_{0.60}Sn_{0.40})_{0.95}Ti_{0.05}O_3$ antiferroelectric bulk ceramics, J. Am. Ceram. Soc. 95 (2012) 1163.

[11] R. Yimnirun, Y. Laosiritaworn, S. Wongsaenmai, S. Ananta, Scaling behavior of dynamic hysteresis in soft lead zirconate titanate bulk ceramics, Appl. Phys. Lett. 89 (2006) 162901.

[12] Y.H. Kim, J.J. Kim, Scaling behavior of an antiferroelectric hysteresis loop, Phys. Rev. B 55 (1997) 11933.

[13] B.H. Ma, M. Narayanan, S. Tong, U. Balachandran, Fabrication and characterization of ferroelectric PLZT film capacitors on metallic substrates, J. Mater. Sci. 45 (2010) 151.

[14] J. Ge, D. Remiens, X. Dong, Y. Chen, J. Costecalde, F. Gao, F. Cao, G. Wang, Enhancement of energy storage in epitaxial $PbZrO_3$ antiferroelectric films using strain engineering, Appl. Phys. Lett. 105 (2014) 112908.

[15] M.H. Lente, A. Picinin, J.P. Rino, J.A. Eiras, 90 degrees domain wall relaxation and frequency dependence of the coercive field in the ferroelectric switching process, J. Appl. Phys. 95 (2004) 2646.

[16] J.M. Liu, H.P. Li, C.K. Ong, L.C. Lim, Frequency response and scaling of hysteresis for ferroelectric $Pr(Zr_{0.52}Ti_{0.48})O_3$ thin films deposited by laser ablation, J. Appl. Phys. 86 (1999) 5198.

[17] R. Yimnirun, Y. Laosiritaworn, S. Wongsaenmai, Effect of uniaxial compressive prestress on ferroelectric properties of soft PZT ceramics, J. Phys. D. Appl. Phys. 39 (2006) 759.

[18] Y.Y. Guo, T. Wei, Q.Y. He, J.M. Liu, Dynamic hysteresis scaling of ferroelectric $Pb_{0.9}Ba_{0.1}(Zr_{0.52}Ti_{0.48})O_3$ thin films, J. Phys. Condens. Matter. 21 (2009) 485901.

[19] X.F. Chen, X.L. Dong, Z.Y. Zhou, J.X. Wang, F. Cao, G.S. Wang, H.L. Zhang, Dynamic hysteresis and scaling behavior for Pb(Zr, Ti)O_3 ceramics, J. Appl. Phys. 115 (2014) 124103.